Received: 25 November 2025 | Revised: 26 January 2026 | Accepted: 25 February 2026 | Published online: 10 March 2026

RESEARCH ARTICLE

Artificial Intelligence and Applications
2026, Vol. 00(00) 1–16
DOI: 10.47852/bonviewAIA62028408

BON VIEW PUBLISHING

Adaptive Footwear Stiffness Driven by Biomechanical Signals for Improving High-Intensity Metabolic-Neuromuscular Performance: A Randomized Controlled Trial

Yining Xu[1,†], Yang Song[1,2,†], Dong Sun[1,*], Zhiyi Zheng[3], Mingwei Sun[3], Wenlong Li[1], Jiachao Cai[1], Xuanzhen Cen[1], Zixiang Gao[4], Liangliang Xiang[5], Monèm Jemni[1,6,7], and Yaodong Gu[1,8,*]

[1] *Faculty of Sports Science, Ningbo University, China*

[2] *Department of Biomedical Engineering, The Hong Kong Polytechnic University, China*

[3] *ANTA Sports Science Laboratory, ANTA (China) Co., Ltd, China*

[4] *Human Performance Laboratory, University of Calgary, Canada*

[5] *Department of Engineering Mechanics, KTH Royal Institute of Technology, Sweden*

[6] *The Carrick Institute, USA*

[7] *Centre for Mental Health Research in Association with the University of Cambridge, UK*

[8] *Research Institute of Sport Science, Hungarian University of Sports Science, Hungary*

Abstract: Background: Basketball shooting performance deteriorates under fatigue, often due to compromised biomechanics and suboptimal footwear stiffness. Footwear with dynamically adjustable longitudinal bending stiffness (LBS) could counteract fatigue effects by maintaining optimal support throughout play. Objective: The objective of this study is to evaluate whether an adaptive LBS basketball shoe—controlled by a machine learning algorithm (logistic regression with support vector machine–recursive feature elimination) using biomechanical signals—can improve high-intensity shooting performance under fatigue compared to the fixed-stiffness footwear. Methods: A total of 60 participants were randomly assigned to high-stiffness (HS), low-stiffness (LS), or self-adaptive stiffness (SS) shoe groups. All completed a 2-min high-intensity shooting and rebounding drill designed to induce fatigue, while real-time kinematic data of the lower limbs and physiological data (heart rate, muscle oxygen saturation) guided SS stiffness adjustments. Results: The SS group achieved significantly more successful shots than the HS and LS groups (mean difference +1.662 vs HS, $p < 0.01$; +2.753 vs LS, $p < 0.001$) and higher shooting accuracy (+0.093 vs HS, $p < 0.01$; +0.117 vs LS, $p < 0.001$). Under fatigue, SS footwear preserved favorable lower-limb joint kinematics (e.g., maximum hip rotation angle +0.234 rad vs HS, $p = 0.014$) without increasing cardiovascular or metabolic demands (no significant differences in heart rate or SmO_2). Conclusion: Adaptive footwear stiffness integrating biomechanical sensing and machine learning improved basketball shooting performance and mitigated fatigue-induced biomechanical degradation, highlighting its potential for enhancing sports performance.

Keywords: lower-limb biomechanics, adaptive footwear stiffness, machine learning, metabolic-neuromuscular coupling task, basketball

1. Introduction

High-intensity skill–physical coupling tasks—characterized by simultaneous high metabolic demand and precise neuromuscular control—are critical determinants of performance in modern team sports. Typical examples include a soccer player sprinting and abruptly cutting to shoot on goal or a basketball player executing consecutive jumps, quick directional changes, and precision shooting under fatigue conditions. Accumulated fatigue during such tasks is known to impair joint mechanics and proprioceptive accuracy, thereby reducing performance and increasing injury risk [1, 2]. Consequently, optimizing mechanical efficiency and protecting against fatigue-induced biomechanical deterioration has emerged as a central challenge in sport biomechanics

***Corresponding authors:** Dong Sun, Faculty of Sports Science, Ningbo University, China. Email: sundong@nbu.edu.cn and Yaodong Gu, Faculty of Sports Science, Ningbo University, China. Email: guyaodong@nbu.edu.cn
[†]**Co-first author**

research. In parallel, recent advances in wearable sensing and embedded intelligence have created opportunities for adaptive sport equipment that can respond to an athlete's state in real time rather than relying on static, one-size-fits-all mechanical designs.

However, previous studies share a critical limitation: they typically assessed fixed footwear stiffness settings during relatively controlled or steady-state tasks such as straight-line running, isolated vertical jumps, or single-angle cutting maneuvers [1–4]. Real-world competitive scenarios are highly dynamic, with physiological states and movement patterns continuously evolving as fatigue accumulates. Consequently, a footwear stiffness that is optimal at the beginning of competition may become suboptimal later due to changes in neuromuscular fatigue or metabolic demand—either becoming excessively stiff, thus requiring greater muscular effort, or overly compliant, resulting in diminished propulsion and stability. This gap underscores the potential need for footwear capable of adapting stiffness dynamically in real time to evolving biomechanical and physiological states.

From an artificial intelligence systems perspective, dynamically regulating footwear stiffness can be formulated as an adaptive, human-in-the-loop control problem in which the athlete's biomechanical signals provide continuous feedback for decision-making. In such a closed-loop sensing–inference–actuation pipeline, the system must (i) sense movement-state changes under fatigue, (ii) infer an appropriate parameter update, and (iii) actuate the mechanical adjustment reliably and repeatedly within the time constraints of sport actions. Importantly, these setting favors data-driven controllers that are lightweight and transparent, enabling practical real-time deployment while retaining interpretability for understanding how biomechanical cues drive equipment adaptation.

To address this critical research gap, this study developed a novel smart basketball shoe system equipped with a servo-driven mechanism to dynamically adjust longitudinal bending stiffness (LBS) in response to real-time biomechanical signals. This footwear incorporates instrumented insoles that monitor center-of-mass (CoM) kinematics. Integrated into the footwear, a data-driven control algorithm—constructed using logistic regression and feature selection via support vector machine–recursive feature elimination (SVM-RFE)—determines optimal footwear stiffness adjustments based on athlete-specific biomechanical data. Machine learning-based personalization strategies are gaining prominence in sport technology, facilitating equipment that adapts dynamically to individual athlete characteristics and needs in real time [5]. Similar interpretable learning pipelines have been widely adopted in medical and other performance-critical decision-support settings, highlighting the value of transparent models when decisions must be audited and deployed safely [6, 7].

The primary aim of this study was to evaluate whether dynamically adjustable footwear LBS enhances performance outcomes in a basketball-specific high-intensity metabolic-neuromuscular coupling task (i.e., a 2-min self-shooting and rebounding three-point drill) compared to conventional footwear conditions of fixed high and low-stiffness. It is hypothesized that adaptive footwear stiffness would, on the one hand, significantly increase successful shot count and shooting accuracy and, on the other hand, maintain favorable lower-limb biomechanical characteristics under fatigue conditions, without imposing additional cardiovascular or metabolic burdens. Demonstrating these effects would establish a new footwear design paradigm-to-equipment that actively adapts to an athlete's physiological states rather than remaining static and potentially broaden applications for performance enhancement and injury mitigation in diverse sports contexts. In addition, this study provides a practical example of an interpretable, biomechanical-signal-driven adaptive control approach for real-time personalization of sports equipment parameters.

2. Related Work

This section reviews evidence on LBS in sport footwear and summarizes limitations of fixed-stiffness designs that motivate an adaptive solution. Footwear design represents a practical and impactful strategy for modulating lower-limb biomechanics and performance outcomes [3, 4]. A crucial footwear feature is LBS, defined as the resistance of the shoe sole to bending around the metatarsophalangeal (MTP) joints. Adjustments in LBS can significantly influence energy storage and return mechanisms, joint work distribution, and overall movement stability. Previous lab-based studies have demonstrated performance benefits of tuning LBS. For instance, increasing footwear stiffness with embedded carbon fiber plates reduced energy loss at MTP joints and improved vertical jump height [4], while optimal midsole stiffness enhanced running economy by 1–4% in distance running [3, 8].

Moreover, appropriate midsole stiffness also contributes to injury prevention. Research by Worobets and Wannop [4] indicates that tailored stiffness can moderate plantar-flexion moments and minimize excessive joint motions, thereby reducing overuse injuries. Basketball-specific evaluations suggest that stiffer midsoles can decrease forefoot deformation, allowing athletes to perform sprinting and cutting movements faster without compromising jump performance and simultaneously lowering peak MTP joint flexion moments linked to stress injuries [4]. Collectively, existing evidence supports the dual benefits of footwear stiffness optimization: enhancing sport performance and reducing biomechanical injury risk.

Overall, prior findings support the benefits of LBS tuning for performance and injury mitigation, but most studies evaluate fixed stiffness under controlled tasks. In real competitive play, fatigue and movement demands evolve rapidly, suggesting the need for footwear that can adapt stiffness in real time.

3. Proposed Methodology

3.1. Contributions and overview

This study designed a smart basketball footwear system capable of real-time adjustment of LBS via a servo-driven mechanism. Moreover, this study proposed a biomechanical-signal-driven closed-loop control framework that maps real-time kinematics to stiffness commands for individualized adaptation. Besides, this study developed an interpretable machine learning decision module (feature selection + logistic regression + SHAP/nomogram) to support transparent stiffness adjustment. At last, this study validated the proposed system in a randomized controlled trial under a high-intensity metabolic-neuromuscular coupling task, assessing shooting performance and fatigue-related biomechanics.

3.2. Self-adaptive stiffness footwear system

The LBS was defined as the resistance of the footwear midsole to forefoot bending deformation during dynamic movements, which reflects the mechanical constraint around the MTP region. In the proposed footwear, LBS was modulated by translating

embedded carbon-fiber strips along predefined tracks within the midsole. A servo-driven mechanism was integrated into the shoe to precisely position the carbon strip, thereby enabling continuous stiffness modulation through a position–stiffness mapping. The mapping between carbon-strip position (expressed as a percentage of the track length) and the effective LBS was pre-calibrated and is reported together with the system overview (Figure 1; calibration details are provided in Section 4).

The servo motor was remotely commanded through a wireless communication module, and the position commands were executed by the onboard actuation mechanism to achieve the desired strip displacement. Such wireless communication and closed-loop actuation are widely adopted in intelligent footwear and wearable systems for real-time human–device interaction [9]. During operation, real-time biomechanical signals were acquired and processed by the control software, which inferred the target stiffness state and issued corresponding position commands to the actuator. In this work, the stiffness-setting decision was driven by the learning module described in Section 3.4, allowing the footwear to adjust LBS in response to the athlete's movement state (Figure 1(c)).

3.3. Biomechanical-signal-driven control framework

The proposed control framework aims to dynamically adjust footwear LBS in real time by converting wearable-sensor motion signals into stiffness-setting commands. Motion data were acquired using the Xsens DOT sensor, a lightweight wearable inertial measurement unit (IMU) integrating a 3-axis accelerometer, gyroscope, and magnetometer, capable of streaming attitude and motion information via Bluetooth Low Energy [10, 11]. The DOT signals provide the kinematic basis for extracting biomechanical descriptors that characterize movement execution and fatigue-related alterations.

The control pipeline consists of four stages: (i) data acquisition, (ii) preprocessing and feature extraction, (iii) model inference, and (iv) actuation command generation. First, raw inertial signals (e.g., acceleration and angular velocity time-series, optionally complemented by magnetometer signals [11]) are captured and segmented into analysis windows aligned with the movement cycle. Second, preprocessing is applied to improve signal quality and feature stability. A low-pass filtering strategy is used to attenuate high-frequency noise prior to feature extraction [12, 13]. After feature computation, feature scaling/standardization is performed to mitigate unit and magnitude discrepancies across variables, which is beneficial for stable inference in linear and margin-based learners [13]. These steps improve robustness to sensor noise and reduce spurious variance that may degrade generalization [10, 13].

Third, the extracted features are fed into a trained decision model to estimate the desired stiffness state. In this study, feature selection was conducted offline using SVM-RFE to identify the most informative biomechanical predictors [14]. The selected feature subset is then used by the logistic regression decision module described in Section 3.4 to compute an interpretable estimate of task success likelihood (or an equivalent decision score), which is subsequently mapped to a target LBS level. Finally, the target LBS level is converted into actuator position commands according to the pre-calibrated position–stiffness mapping (Figure 1(b)), and the servo mechanism updates the carbon-strip position to realize adaptive stiffness control.

3.4. Learning and explainability module

An interpretable learning module was developed to support transparent, athlete-specific stiffness adjustment. We adopted logistic regression to model the relationship between biomechanical predictors and binary shooting outcomes (success/failure), given its interpretability, low computational overhead, and suitability for

Figure 1

Process of footwear LBS adjustment. (a) structure of the footwear; (b) relationship between the carbon strip's position and the footwear's LBS; (c) process of the LBS setting driven by real-time biomechanical signals

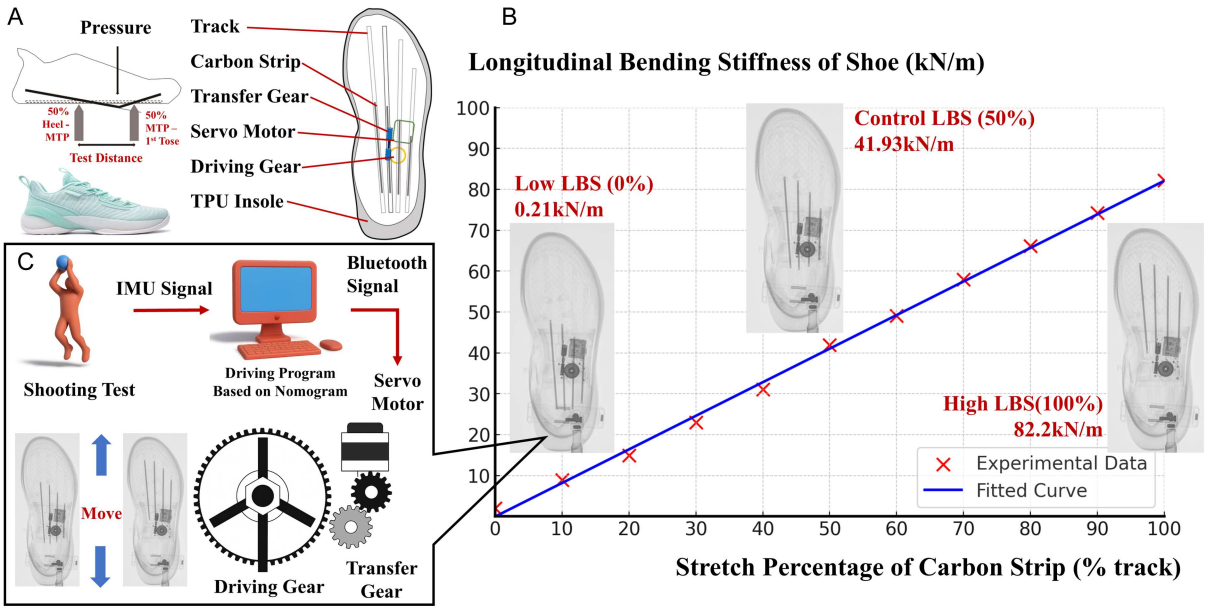

dichotomous outcomes frequently encountered in sports biomechanics. Candidate predictors were derived from CoM kinematics and lower-limb biomechanical descriptors that are theoretically linked to shooting stability and fatigue-induced execution changes (e.g., movement timing characteristics, CoM displacement/velocity patterns, and segmental/joint kinematic descriptors).

To reduce redundancy and mitigate multicollinearity in high-dimensional biomechanical feature sets, an embedded feature-selection step was applied using SVM-RFE, which iteratively removes features with low contribution to margin-based separation and is widely used for robust variable selection in complex datasets [14]. The resulting compact feature subset was then used to fit the final logistic regression model that outputs an individualized probability (or decision score) for shooting success. To enhance interpretability beyond coefficient signs and magnitudes, feature contributions were quantified using Shapley Additive Explanations (SHAP), which attributes the model's prediction to individual features in a consistent additive manner [8, 15, 16]. The final logistic regression model was further visualized as a nomogram to facilitate real-time use by converting feature values into an intuitive score and corresponding success likelihood, thereby enabling a transparent rule for stiffness-setting decisions during adaptive control.

4. Experimental Section

4.1. Participants

A priori power analysis (G*Power 3.1, ANOVA repeated measures, between factors) indicated that 18 participants per group would provide 80% power ($\alpha = 0.05$) to detect a large effect size ($f = 0.40$) in the primary outcome (successful shot count) [16]. Therefore, 60 healthy college basketball athletes (28 males and 32 females, age: 18–22 years) were recruited from Ningbo University and randomly allocated (computer-generated block randomization, block size = 3, concealed envelopes) in equal numbers ($n = 20$) to one of three footwear conditions: high-stiffness footwear (HS, 82.2 kN/m), low-stiffness footwear (LS, 0.21 kN/m), or self-adaptive stiffness footwear (SS, baseline 41.9 kN/m with algorithm-driven adjustments). Randomization was performed using SPSS version 26 (IBM, IL, USA), ensuring balanced distribution of gender and age among groups. Eligibility criteria were as follows:

1) age between 18 and 22 years;
2) no known endocrine, metabolic, neuromuscular, or musculoskeletal disorders, and no medical restrictions for vigorous physical activity;
3) no history of musculoskeletal injury within the last 6 months;
4) right-handed.

4.2. Study design

This study utilized a randomized controlled trial design. Participants performed a high-intensity metabolic-neuromuscular coupling task—specifically, a standardized 2-min self-shooting and rebounding three-point basketball shooting drill [17]. All participants completed an initial pre-test session wearing standardized medium LBS footwear (control condition, LBS = 41.93 kN/m). The pre-test included two repetitions of the 2-min task with a 10-min rest interval, with the better of the two attempts selected for subsequent modeling purposes. Participants then rested for 24 h without additional physical activity or training. Following this rest period, participants returned for the post-test session, during which each participant completed the same 2-min task once, wearing their randomly assigned footwear conditions (HS, LS, or SS).

Blinding procedures were implemented: all footwear types were visually identical, and participants were not informed about the specific stiffness conditions, thereby achieving a single-blind experimental design.

4.3. Experimental protocol

The flow diagram of the study is shown in Figure 2. All experimental procedures were conducted in a standardized indoor basketball court. Participants were required to arrive at the laboratory at the same time of day for both pre-test and post-test sessions to control circadian influences on performance. Room temperature was consistently maintained between 20 and 23 °C, and relative humidity was controlled at approximately 50–60%.

Upon arrival at the laboratory for the pre-test session, participants were fitted with the control footwear and equipped with sensors for monitoring biomechanical and physiological signals. After sensor calibration, participants performed a standardized 10-min warm-up routine, including dynamic stretching, cardiovascular activation (such as jogging and jumping jacks), and dynamic movements activating major muscle groups (e.g., squats, lunges, arm circles). The warm-up was standardized to ensure participants reached approximately 60% of their estimated maximum heart rate (HR) (calculated as 220 minus age).

Following the warm-up, participants engaged in 10 min of free three-point shooting practice to familiarize themselves with the testing environment and equipment. Immediately thereafter, participants performed two separate 2-min trials of the self-shooting and rebounding three-point basketball drill, with a 10-min seated rest interval between trials. During each 2-min trial, participants continuously attempted three-point shots, retrieved their own rebounds, and returned quickly to the three-point line to attempt the next shot. The rules of the test were as follows:

1) The tests use a size 7 basketball (Type: GG7, Kabushiki-gaisha Moruten, Japan).
2) Participants' lower extremities must not employ any form of joint stabilization, including but not limited to tape bindings, kinesiology tape, or any protective equipment that offers support and reinforcement.
3) The test commences and concludes with the resounding beep of a 24-second timer.
4) There is no violation for out-of-bounds, traveling, or double dribbling; the only rule is that at each three-point shot, the participant's feet must be outside the three-point line.

Each trial performance was quantified based on the total number of shooting attempts and successful shots made. The best performance trial (based on successful shots and shooting accuracy) was selected for subsequent algorithm development and modeling.

In the post-test session (conducted exactly 24 h later), participants returned and repeated the identical warm-up and familiarization shooting practice. Immediately afterward, each participant completed the 2-min self-shooting and rebounding three-point drill once, while wearing footwear corresponding to their randomized experimental groups (HS, LS, or SS). Participants remained blind to their footwear condition, ensuring consistency of motivation and effort across groups. Researchers administering the task were also blinded to the footwear conditions (double-blind approach), further minimizing bias in data collection and outcome assessment.

Figure 2
The flow diagram of the study

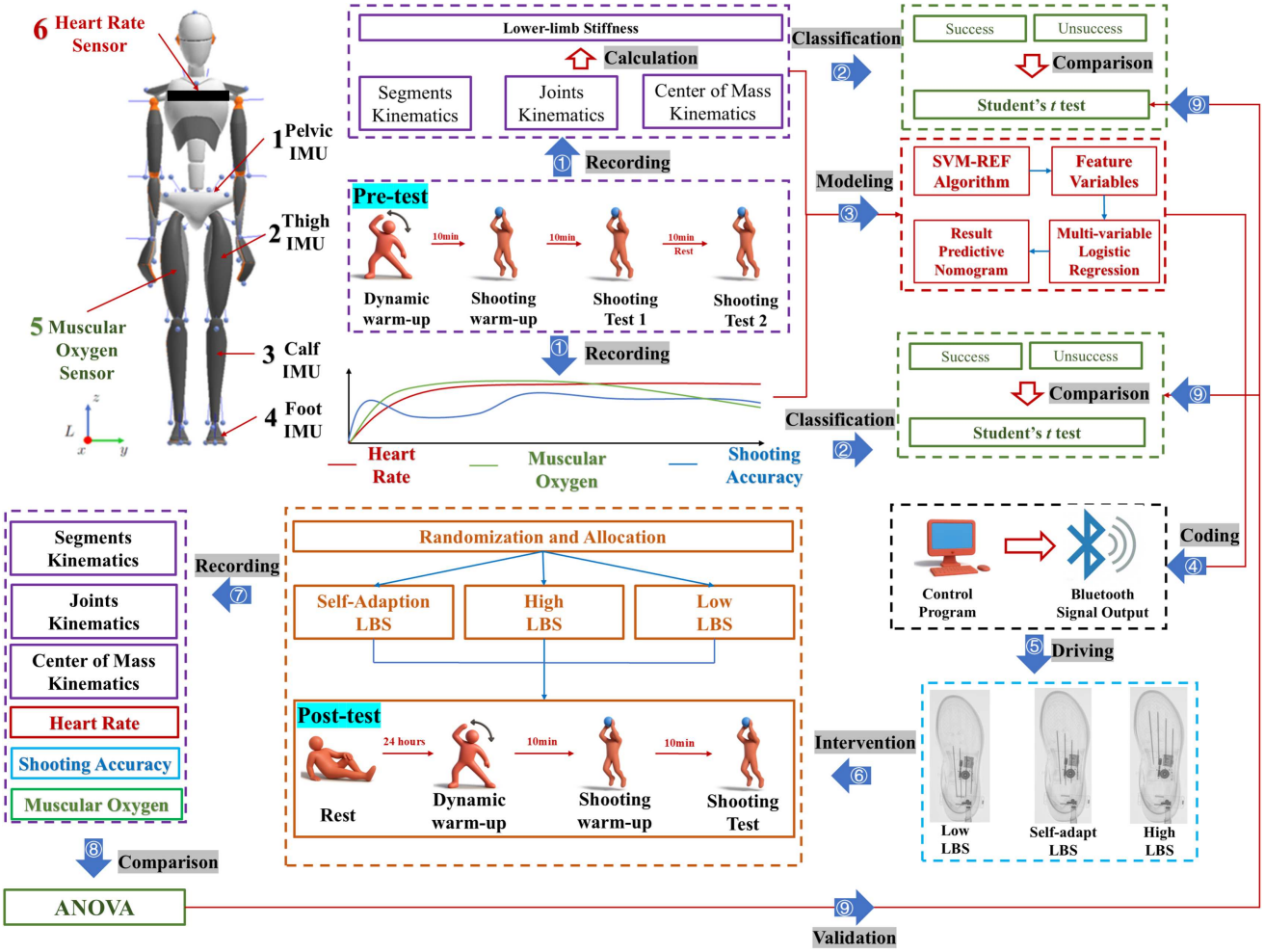

Throughout both pre- and post-test trials, biomechanical and physiological data—including CoM kinematics, lower-limb joint angles and angular velocities, HR, and muscle oxygen saturation (SmO_2)—were continuously recorded. Data acquisition procedures were identical across all sessions and groups to maintain consistency and comparability.

4.4. Instrumentation and system calibration

Three-dimensional kinematic data were collected using IMU sensors. A pelvis-mounted Xsens DOT IMU system (Movella Technologies B.V., Netherlands) was used to capture kinematics serving as a proxy for participants' CoM motion, while lower-limb joint kinematics (joint angles and angular velocities) were recorded using the Xsens MVA motion capture system (Movella Technologies B.V., Netherlands). Both systems were configured to operate at a sampling frequency of 100 Hz. IMU-based kinematic acquisition and analysis have been widely adopted in non-laboratory sport settings [10], and the Xsens DOT platform provides real-time wearable sensing suitable for such applications [11].

Footwear stiffness calibration and experimental settings. The relationship between carbon-strip position (expressed as a percentage of the total track length) and footwear LBS was established via a three-point bending calibration test (Figure 1(b)). The position–LBS mapping was confirmed to be approximately linear (Figure 1(b), $R^2 > 0.95$), enabling stiffness control through actuator-driven strip translation. In the high-stiffness (HS) condition, the carbon strips were fully extended (100% of track length; LBS = 82.2 kN/m). In the low-stiffness (LS) condition, the strips were completely retracted (0% of track length; LBS = 0.21 kN/m). The control footwear used during the pre-test had the carbon strips fixed at the midpoint of the track (LBS = 41.93 kN/m). For the self-adaptive stiffness (SS) condition, stiffness was updated between shooting attempts based on real-time biomechanical signal input and the predefined control protocol driven by the trained logistic regression decision model.

HR data were continuously recorded using a Polar H10 chest-strap HR sensor (Polar Electro Oy, Kempele, Finland). The device transmitted HR signals via Bluetooth to the acquisition system at 1-s intervals, supporting computation of maximum, minimum, and average heart rates during the task [18].

Local SmO_2 data were obtained using a Humon Hex near-infrared spectroscopy muscle oxygenation sensor (Humon Inc., United States). The sensor was placed on the thigh of the participants' dominant leg and recorded continuously at 1 Hz throughout the testing session [19].

4.5. Data processing and biomechanical variables

All kinematic signals were time-aligned prior to analysis. CoM-related kinematic variables derived from the Xsens DOT stream and lower-limb joint kinematics derived from the Xsens MVA system were synchronized using acquisition timestamps and analyzed at the configured sampling frequency (100 Hz). To improve robustness of derived features, preprocessing steps were applied to attenuate high-frequency noise in inertial signals prior to feature extraction (e.g., low-pass filtering) [12, 13], followed by feature scaling/standardization where appropriate to improve numerical stability for downstream modeling [13].

Each shooting cycle was segmented into eccentric contraction (EC) and concentric contraction (CC) phases using CoM vertical velocity and vertical position criteria (Figure 3). The resulting phase boundaries were then applied to partition (i) CoM kinematics and (ii) joint kinematics (angles and angular velocities) into EC/CC segments on a per-cycle basis, ensuring consistent phase-specific feature computation across sensor modalities.

Biomechanical variables were defined and computed as follows: EC and CC durations (t_{EC} and t_{CC}) were computed from the segmented phase boundaries; CoM vertical displacements during EC and CC (D_{EC} and D_{CC}) were computed from the CoM vertical position signal within each phase; and phase-specific lower-limb stiffness indices (LS_{EC} and LS_{CC}) were computed based on the relationship between the vertical ground reaction force term (F_G) and the corresponding CoM vertical displacement within EC and CC, respectively. The complete computation procedure and symbol definitions are provided in Equations (1) to (5), and the EC/CC partitioning workflow is illustrated in Figure 3.

$$a_{i(j)} = \frac{v_{i(j)+1} - v_{i(j)}}{1/f} \tag{1}$$

$$F_{G,i(j)} - mg = ma_{i(j)} \tag{2}$$

$$d_{i(j)} = \frac{1}{2}(v_{i(j)+1} - v_{i(j)})(1/f) \tag{3}$$

$$D_{EC} = \sum_{i=1}^{n} d_i, \quad D_{DC} = \sum_{j=1}^{m} d_j \tag{4}$$

$$LS_{EC} = \frac{\sum_{i=1}^{n} F_{G,i}}{n \bullet D_{EC}}, \; LS_{CC} = \frac{\sum_{j=1}^{m} F_{G,j}}{m \bullet D_{CC}} \tag{5}$$

4.6. Modeling training, validation, and statistical analysis

Statistical analyses were performed using IBM SPSS Statistics (version 26, IBM Inc., IL, USA) and R (version 4.1.2; R Foundation for Statistical Computing, Vienna, Austria). Data normality was examined using the Shapiro–Wilk test, and homogeneity of variances was assessed using Levene's test prior to parametric analyses. The nominal significance level was set at $\alpha = 0.05$. When assumptions for parametric tests were violated, nonparametric alternatives were used as specified below. For multiple comparisons, the Bonferroni correction was applied to control family-wise error rates.

During the pre-test phase, shooting attempts were labeled as succeeded or failed. Group-invariant baseline descriptors (e.g., HR, SmO_2, demographics, and kinematic variables) were compared between succeeded and failed attempts using independent-samples *t*-tests (for normally distributed data) or Mann–Whitney *U* tests (for non-normally distributed data), with Bonferroni-adjusted thresholds applied as needed.

During the post-test phase, between-group comparisons across footwear conditions (HS, LS, and SS) were conducted using one-way ANOVA for normally distributed variables or Kruskal–Wallis *H* tests otherwise. Significant omnibus effects were followed by pairwise post hoc comparisons with Bonferroni

Figure 3

Data partitioning process of EC and CC phases. (a) step 1: preliminary data partitioning based on velocity of CoM collected by Xsens Dot; (b) step 2: preliminary data partitioning of CoM position based on results of step 1; (c) step 3: movement cycle correction based on the results of step 2 and the distinction between EC and CC phases; (d) step 4: joint kinematic data (collected by Xsens MVA) partitioning based on the result of step 3

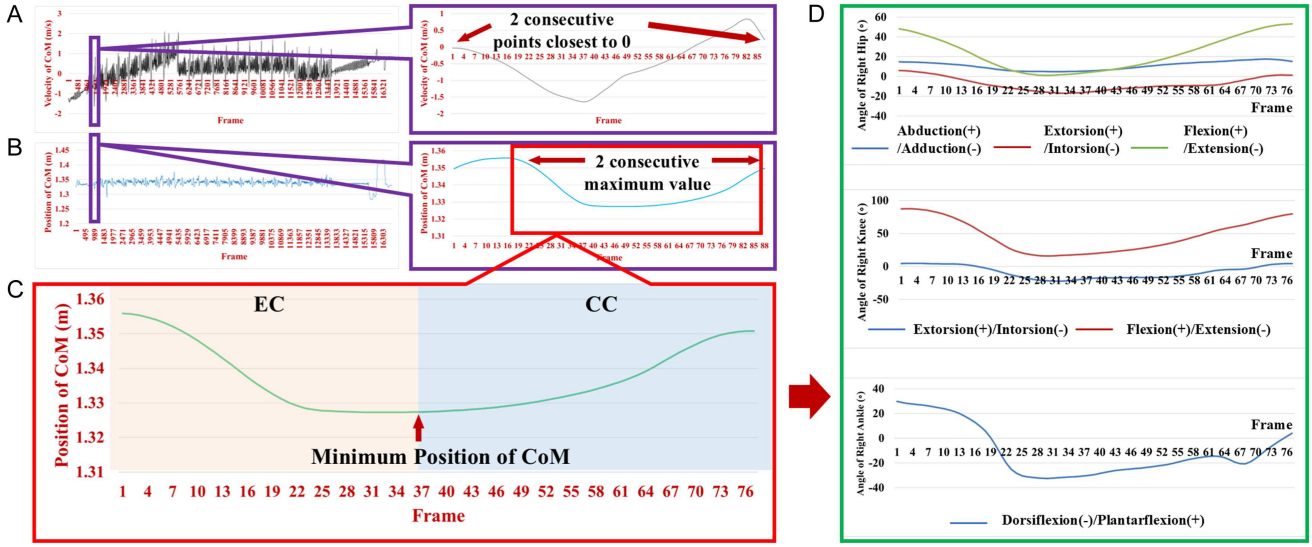

correction; for three-group pairwise testing, the adjusted significance threshold was defined as $p < 0.0167$ (0.05/3). Effect sizes were reported as partial eta-squared (η^2) for ANOVA and Cohen's d for pairwise comparisons where applicable. Continuous outcomes were summarized using means with 95% confidence intervals, and standard deviations were also reported to indicate dispersion.

A logistic regression model was trained using pre-test biomechanical predictors to estimate the probability of successful shooting to reflect the common trade-off between interpretability and nonlinear model capacity in performance-critical applications, where transparent decision rules can be preferable for deployment and verification [20]. Candidate variables were first screened via univariate logistic regressions with a sensitivity threshold of $\alpha = 0.1$. To reduce redundancy and mitigate multicollinearity, feature selection was performed using SVM-RFE. Feature-selection-driven, interpretable pipelines have also been reported to generalize well in applied AI systems, supporting the methodological rationale of combining logistic regression with SVM-RFE [14, 21]. Model generalization was evaluated through an external validation split (training 70%, validation 30%). Within the training set, 10-fold cross-validation was performed to assess robustness and support stable feature selection. In addition, feature-selection stability across folds was summarized using selection-frequency statistics to complement performance-based validation [22]. The held-out validation set was evaluated using bootstrap resampling (1000 iterations) to quantify performance metrics, including area under curve (AUC), accuracy, sensitivity, and specificity. Model interpretability was further enhanced using SHAP to quantify feature contributions [15], and the finalized logistic regression model was presented as a nomogram to facilitate deployment as a transparent decision aid for stiffness-setting. Moreover, to further validate the contribution of the selected biomechanical feature set, a leave-one-feature-out ablation analysis was performed.

To examine the biomechanical plausibility and consistency of the adaptive control strategy, lower-limb kinematic variables identified as key predictors during the pre-test model development were re-examined across post-test footwear conditions. Directional consistency between pre-test discriminative patterns (succeeded vs failed attempts) and post-test group differences (SS vs fixed stiffness) was used as a qualitative validation criterion for the model-derived stiffness adjustments under fatigue conditions.

The control and inference pipeline was implemented in Python (Python 3.7). IMU data access and real-time streaming were implemented using the Xsens DOT software interface and platform resources [13]. Feature processing and model inference were implemented using SciPy/Numpy for signal processing and matrix computation and scikit-learn for loading the trained SVM-RFE feature-selection pipeline and the fitted logistic regression model [16]. The deployment can run on standard computing platforms (e.g., laptops or embedded systems). Sensor–host communication was established via Bluetooth Low Energy, and actuator control commands were sent through standard device interfaces. The Xsens DOT supports configurable output rates (nominally 60–120 Hz depending on mode) [13]; in this study, kinematic acquisition was configured to match the experimental sampling setup. Overall, the implementation integrates IMU-based sensing [10], feature processing, and machine learning inference to support adaptive stiffness control for changing task demands [13, 14, 23].

4.7. Results

4.7.1. Pre-test kinematic differences and model features

Pre-test analyses compared successful and failed shooting attempts to identify discriminative biomechanical features for subsequent predictive modeling. As shown in Table 1, no significant differences were observed between outcomes in demographic characteristics or physiological variables, including sex, age, height, BW, body mass index (BMI), body fat percentage (BF%), muscle mass percentage (Muscle%), total shooting attempts, average heart rate (AHR), or average SmO_2 ($p > 0.05$).

Table 1
Baseline characteristics (mean [95% confidence intervals])

Items	All (n = 1233)	Failed (n = 571)	Succeeded (n = 662)	p-value
AHR (bpm)	140.00 (124.00, 156.00)	140.00 (124.00, 156.00)	140.00 (124.00, 155.00)	0.565
SmO_2 (%)	55.00 (47.00, 63.00)	54.00 (47.00, 63.00)	56.00 (48.00, 63.00)	0.300
t_{EC} (ms)	642.00 (568.20, 708.60)	586.80 (548.70, 619.80)	704.70 (671.40, 742.05)	< 0.001
t_{CC} (ms)	709.92 (637.16, 799.00)	805.80 (760.92, 844.56)	671.84 (625.94, 707.20)	< 0.001
t_{EC}/t_{CC}	0.94 (0.74, 1.06)	0.74 (0.70, 0.77)	1.05 (1.00, 1.12)	< 0.001
D_{EC} (cm)	8.10 (7.50, 8.50)	8.10 (7.60, 8.60)	8.10 (7.50, 8.50)	0.253
D_{CC} (cm)	10.01 (9.60, 10.70)	10.10 (9.60, 10.70)	10.10 (9.60, 10.70)	0.567
D_{EC}/D_{CC}	0.79 (0.75, 0.84)	0.80 (0.75, 0.85)	0.79 (0.74, 0.84)	0.326
LS_{EC} (kN/m)	9.69 (8.80, 13.60)	13.78 (13.15, 14.31)	8.89 (8.44, 9.33)	< 0.001
LS_{CC} (kN/m)	9.86 (6.89, 10.75)	6.89 (6.48, 7.24)	10.68 (10.20, 11.17)	< 0.001
LS_{EC}/LS_{CC}	0.94 (0.83, 1.99)	2.01 (1.90, 2.12)	0.83 (0.78, 0.88)	< 0.001

Note: Numeric data is presented as mean (95% confidence intervals); EC: eccentric contraction; CC: concentric contraction; BW: body weight; BMI: body mass index; FR (body fat%): participants' body fat percentage; MR (muscle mass%): participants' skeletal muscle mass percentage; AHR (Avg. HR): average heart rate during the task; SmO_2: average muscle oxygen saturation; t_{EC}: duration of the eccentric contraction phase; t_{CC}: duration of the concentric contraction phase; DEC: vertical displacement of CoM during the EC phase; DCC: vertical displacement of CoM during the CC phase; LS_{EC}: average lower-limb stiffness during the EC phase; LS_{CC}: average lower-limb stiffness during the CC phase.

In addition, no significant differences were found in CoM vertical displacement metrics during the eccentric (D_{EC}) and concentric (D_{CC}) phases, nor in the D_{EC}/D_{CC} ratio ($p > 0.05$).

In contrast, several temporal and stiffness-related variables differed significantly between outcomes. Successful attempts exhibited longer EC durations (t_{EC}: 704.70 ms vs 586.80 ms, $p < 0.001$), shorter concentric contraction durations (t_{CC}: 671.84 ms vs 805.80 ms, $p < 0.001$), and higher t_{EC}/t_{CC} ratios (1.05 vs 0.74, $p < 0.001$). Successful attempts also showed lower average lower-limb stiffness during the eccentric phase (LS_{EC}: 8.89 kN/m vs 13.78 kN/m, $p < 0.001$), higher stiffness during the concentric phase (LS_{CC}: 10.68 kN/m vs 6.89 kN/m, $p < 0.001$), and lower LS_{EC}/LS_{CC} ratios (0.83 vs 2.01, $p < 0.001$).

Supplementary Material S2 provides detailed comparisons of lower-limb joint kinematics. Most joint angle and angular velocity variables did not differ significantly between successful and failed attempts ($p > 0.05$), suggesting limited discriminative value of these joint-level parameters for immediate shooting success in the present dataset.

Using SVM-RFE with 10-fold cross-validation, three variables were identified as the most predictive features: LS_{EC}/LS_{CC} ratio, LS_{EC}, and t_{EC}/t_{CC} ratio (Figure 4(a–b)). The logistic regression model based on these predictors was visualized as a nomogram (Figure 4(c)) and used to guide stiffness-setting decisions during the SS condition. Model discrimination is summarized by receiver operating characteristic (ROC) curves for the training and validation sets (Figure 4(d–e)), yielding AUC values of 0.792 and 0.837, respectively, indicating good predictive performance with limited evidence of overfitting. Detailed ablation results are reported in Table 2. According to Table 2, the full model provided the most balanced performance across metrics (AUC 0.837, sensitivity 0.857, and specificity 0.857). After using

Figure 4
The outcome of feature selection. (a) Root Mean Squared Error (RMSE) under 10-fold cross-validation within the number of variables; (b) variable importance based on SHAP-value; (c) nomogram of the results prediction and performance optimization; (d) ROC curve of the training set; (e) ROC curve of the validation set

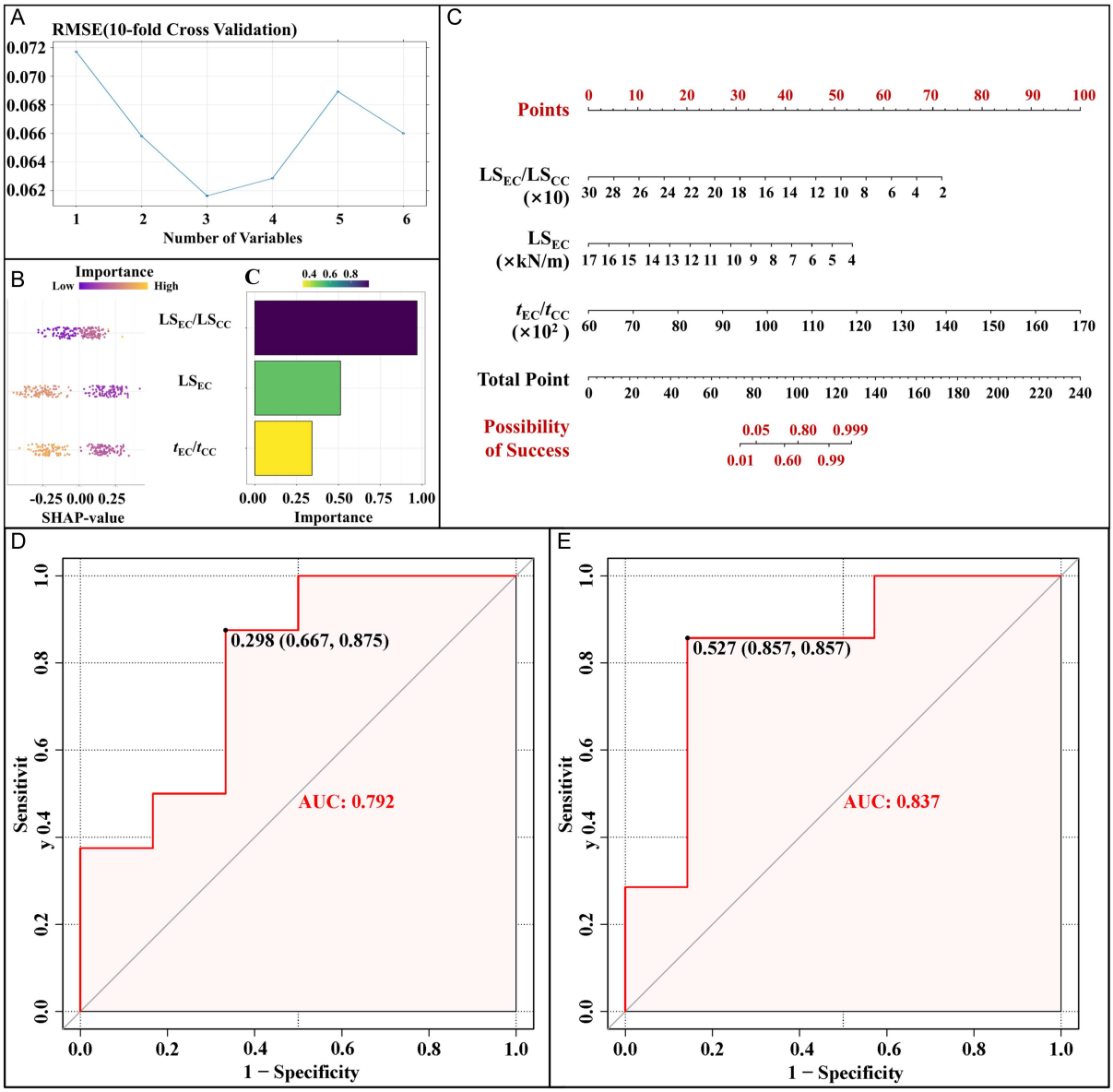

Table 2
Leave-one-feature-out ablation of the final logistic regression model

Model	AUC	Cut-off threshold	Sensitivity	Specificity
Full model	0.837	0.527	0.857	0.857
Remove LS_{EC}/LS_{CC}	0.796	0.275	1.000	0.571
Remove LS_{EC}	0.816	0.369	0.714	0.857
Remove t_{EC}/t_{CC}	0.796	0.564	0.857	0.714

the same 70/30 external split and evaluation protocol, removing LS_{EC}/LS_{CC} resulted in a lower AUC (0.796) and specificity (0.571), removing LS_{EC} resulted in a lower AUC (0.816) and specificity (0.714), whereas removing t_{EC}/t_{CC} reduced AUC (0.796) and specificity (0.714).

4.7.2. Participants' characteristics and performance comparison

Participants' demographic characteristics, physiological parameters, and performance outcomes across the three footwear conditions (HS, LS, and SS) are summarized in Table 3. No significant differences were observed among groups regarding sex distribution, age, height, body weight (BW), BMI, body fat percentage (BF%), muscle mass percentage (Muscle%), total shooting attempts, maximum heart rate (Max. HR), minimum heart rate (Min. HR), AHR, maximum muscle oxygen saturation (Max. SmO_2), minimum muscle oxygen saturation (Min. SmO_2), or average muscle oxygen saturation (Avg. SmO_2) ($p > 0.05$).

However, significant group differences emerged in shooting performance outcomes, specifically the number of successful shooting attempts and shooting accuracy. ANOVA revealed significant overall differences in successful shot counts [F (2, 57) = 12.36, $p < 0.001$, partial $\eta^2 = 0.30$] and accuracy [F (2, 57) = 15.44, $p < 0.001$, partial $\eta^2 = 0.35$].

Post hoc analyses (Table 4) further indicated that the SS group achieved significantly higher numbers of successful shooting attempts (mean difference = +1.662, $p < 0.01$ vs HS; mean difference = +2.753, $p < 0.001$ vs LS) and higher shooting accuracy (mean difference = +0.093, $p < 0.01$ vs HS; mean difference = +0.117, $p < 0.001$ vs LS). No significant differences were detected between HS and LS groups for either successful attempts (mean difference = +1.091, $p = 0.312$) or accuracy (mean difference = +0.024, $p = 0.635$).

Table 3
Participants' characteristics and performance comparison

Items	All ($n = 60$)	HS ($n = 20$)	LS ($n = 20$)	SS ($n = 20$)	$F(\chi^2)$	p-value
Sex					1.71	0.419
Male	28 (46.67%)	10 (50.00%)	7 (35.00%)	11 (55.00%)		
Female	32 (53.33%)	10 (50.00%)	13 (65.00%)	9 (45.00%)		
Age (year)	21.00 (19.00, 22.25)	20.00 (18.75, 21.25)	22.00 (19.75, 23.00)	20.50 (18.00, 22.25)	1.629	0.183
Height (cm)	178.50 (172.00, 187.00)	179.00 (172.50, 187.00)	177.00 (172.50, 184.25)	178.50 (172.00, 195.50)	0.133	0.963
BW (kg)	81.25 (77.31, 85.20)	83.10 (76.80, 89.38)	80.05 (73.14, 86.96)	80.63 (72.23, 89.02)	0.256	0.804
BMI (kg/m^2)	25.00 (22.00, 27.00)	25.40 (24.00, 27.00)	24.63 (23.00, 27.00)	23.00 (22.00, 26.50)	0.860	0.393
FR (% BW)	19.38 (18.19, 20.58)	18.10 (16.16, 20.04)	20.65 (18.50, 22.80)	19.40 (17.09, 21.72)	1.674	0.220
MR (% BW)	44.00 (40.00, 47.00)	44.50 (41.75, 47.75)	41.50 (38.75, 46.25)	45.00 (40.00, 47.00)	1.344	0.222
Attempt (times)	21.00 (20.00, 22.00)	21.00 (20.00, 22.25)	20.00 (19.00, 21.25)	21.00 (19.75, 22.00)	1.603	0.138
Succeeded (times)	11.07 (10.51, 11.70)	10.88 (9.98, 11.82)*	9.79 (8.86, 10.74)*	12.54 (11.62, 13.58)	9.523	<0.001
Accuracy	0.52 (0.47, 0.60)	0.50 (0.46, 0.57)*	0.48 (0.43, 0.51)*	0.60 (0.56, 0.65)	17.141	<0.001
Max. HR (bpm)	169.00 (167.00, 170.00)	169.00 (167.00, 170.00)	169.00 (168.00, 170.00)	168.50 (166.00, 169.25)	0.988+	0.360
Min. HR (bpm)	109.00 (108.00, 111.25)	109.00 (109.00, 110.00)	109.00 (108.00, 112.00)	109.50 (108.00, 111.50)	0.162+	0.942

(*Continued*)

Table 3
(*Continued*)

Items	All (n = 60)	HS (n = 20)	LS (n = 20)	SS (n = 20)	$F(\chi^2)$	p-value
Avg. HR (bpm)	139.45 (138.38, 140.52)	140.58 (138.65, 142.52)	139.35 (137.99, 140.72)	138.42 (136.06, 140.78)	1.148	0.259
Max. SmO_2 (%)	69.00 (69.00, 70.00)	69.50 (69.00, 70.00)	69.00 (69.00, 70.00)	69.50 (69.00, 70.00)	0.060$^+$	0.961
Min. SmO_2 (%)	41.00 (40.00, 41.00)	40.00 (40.00, 41.00)	41.00 (40.00, 41.00)	41.00 (40.75, 42.25)	0.833$^+$	0.122
Avg. SmO_2 (%)	55.16 (54.74, 55.58)	55.17 (54.35, 55.99)	55.20 (54.43, 55.97)	55.11 (54.39, 55.83)	0.017	0.984

Note: Frequency data is presented as case (%), the difference between groups applied the Kruskal–Wallis test; numeric data is presented as mean (95% confidence intervals), the difference between groups used ANOVA; *: have statistically significant difference when being compared to SS; +: the p-value of ANOVA based on Welch's F test because the p-value of Shapiro–Wilk test lower than 0.05, meaning that the data does not conform to a normal distribution; BW: body weight; BMI: body mass index; FR: fat rate; MR: muscle rate; HR: heart rate; SmO_2: muscle oxygen saturation.

Table 4
Results of the post hoc test of the variables with significant differences

Items	Group	LS	SS
Succeeded (times)	HS	1.09 (1.72)	–1.66 (–2.65)*
	LS	/	–2.75 (–4.37)*
Accuracy (%)	HS	0.02 (1.07)	–0.09 (–4.15)*
	LS	/	–0.12 (–5.22)*

Note: The data in the table is the mean difference of groups in row and column with its t-value in the post hoc test; *: mean difference of groups in row and column reached statistical significance ($p < 0.0167$).

4.7.3. Validation of the adaptive footwear LBS algorithm

The validation of the adaptive footwear LBS algorithm was performed by analyzing lower-limb joint angles (Table 5) and angular velocities (Table 6). Kinematic variables significantly differing across footwear groups (SS vs HS and LS) in the post-test phase were compared with the pre-test findings to confirm the consistency of adaptive algorithm effects.

For lower-limb joint angle variables (Table 5), significant differences were observed primarily at the hip and knee joints. Specifically, during the EC phase, the SS condition exhibited significantly reduced maximum hip adduction/abduction angle (mean difference = −0.15 rad vs HS, p = 0.004; −0.13 rad vs LS, p = 0.014) and range of hip adduction/abduction motion (mean difference = −0.16 rad vs HS, p = 0.001; −0.14 rad vs LS, p = 0.004) on the dominant leg. On the non-dominant leg, significantly greater hip rotation angles (mean difference = +0.20 rad vs LS, p = 0.012) and ranges of rotation (mean difference = +0.21 rad vs LS, p = 0.007) were found in the SS condition compared to LS.

During the CC phase, significant differences were similarly observed at the hip and knee joints. Notably, maximum hip rotation angles (mean difference = +0.23 rad vs HS, p = 0.014) and minimum knee extension/flexion angles (mean difference = +0.081 rad vs HS, p = 0.015; +0.07 rad vs LS, p = 0.024) differed significantly, favoring biomechanical profiles associated with successful shooting in pre-tests.

Analysis of angular velocity variables (Table 6) showed similar consistency. During the EC phase, the dominant leg in the SS group showed significantly higher average hip adduction/abduction angular velocity (mean difference = +0.72 rad/s vs HS, p = 0.002; +0.64 rad/s vs LS, p = 0.007), and lower maximum hip rotation angular velocity (mean difference = −1.67 rad/s vs HS, p = 0.001). On the non-dominant side, SS demonstrated significantly lower maximum (mean difference = −1.92 rad/s vs HS, p = 0.010) and average hip rotation angular velocities (mean difference = −0.58 rad/s vs HS, p = 0.007).

During the CC phase, significant differences were evident, notably higher maximum knee extension/flexion angular velocity in SS (mean difference = +4.48 rad/s vs HS, p = 0.015), and lower hip adduction/abduction angular velocities on the non-dominant side (mean difference = −3.46 rad/s vs HS, p = 0.008).

Importantly, all significant variables identified in the post-test ANOVA were consistent with pre-test findings comparing successful versus unsuccessful shooting attempts. The directional changes and biomechanical profiles observed under the adaptive footwear condition closely mirrored those identified as favorable predictors in the logistic regression model developed during pre-testing.

4.8. Discussion

This study introduced a logistic regression and SVM-RFE-controlled adaptive LBS footwear system and evaluated it using a high-intensity basketball shooting protocol. The primary objective was to determine whether dynamically modulated shoe stiffness could enhance shooting performance and lower-limb

Table 5
Algorithm validation based on angle (rad) of lower-limb joints

Phase	Left/right	Joint	Kinematic variables	Student's *t*-test			Post hoc test of ANOVA			
				MD(SE)	*t*	*P*	Comparison	MD(SE)	*t*	*P*
EC	Right	Hip	Max.adduction/abduction	–1.02(0.03)	32.65	<0.05	SS-HS	–0.15(0.05)	–2.67	0.004
							SS-LS	–0.13(0.05)	–3.00	0.014
			ROM.adduction/abduction	–1.09(0.02)	45.46		SS-HS	–0.16(0.05)	–3.33	0.001
							SS-LS	–0.14(0.05)	–3.04	0.004
	Left	Hip	Max.rotation	1.80(0.04)	–50.32		SS-HS	0.12(0.08)	1.48	0.127[$]
							SS-LS	0.20(0.08)	2.72	0.012
		Knee	ROM.rotation	1.629(0.043)	–38.22	<0.05	SS-HS	0.11(0.08)	1.34	0.167[$]
							SS-LS	0.21(0.08)	2.88	0.007
			ROM.extention/flexion	–1.017(0.037)	–27.29		SS-HS	–0.15(0.06)	–2.45	0.011
							SS-LS	–0.131(0.058)	–2.41	0.024[$]
CC	Right	Hip	Max.rotation	2.16(0.05)	–44.23		SS-HS	0.23(0.10)	2.27	0.014
							SS-LS	0.22(0.10)	2.92	0.022[$]
			Min.extention/flextion	0.80(0.02)	–53.96	<0.05	SS-HS	0.08(0.03)	2.31	0.015
							SS-LS	0.08(0.03)	2.64	0.024[$]
		Knee	Max.rotation	1.77(0.03)	–54.59		SS-HS	0.17(0.07)	2.25	0.020[$]
							SS-LS	0.20(0.07)	2.91	0.007
	Left	Hip	Min.rotation	1.04(0.02)	–47.76		SS-HS	0.13(0.04)	2.96	0.003
							SS-LS	0.12(0.05)	2.70	0.010
			ROM.rotation	–0.70(0.03)	28.46	<0.05	SS-HS	–0.10(0.04)	–2.59	0.007
							SS-LS	–0.09(0.04)	–2.68	0.020[$]
		Knee	Min.rotation	0.52(0.03)	–15.44		SS-HS	0.07(0.04)	1.57	0.120[$]
							SS-LS	0.11(0.05)	2.62	0.013

Note: EC: eccentric contraction; CC: concentric contraction; MD: mean difference; SE: standard error; Max: maximum; Min: minimum; Ave: average; [$]: without statistically significant difference ($p > 0.0167$).

Table 6
Algorithm validation based on angular velocity (rad/s) of lower-limb joints

				Student's *t*-test			Post hoc test of ANOVA			
Phase	Left/right	Joint	Kinematic variables	MD(SE)	*t*	*p*-value	Comparison	MD(SE)	*t*	*p*-value
EC	Right	Hip	Ave.adduction/abduction	6.47(0.06)	–104.02	<0.05	SS-HS	0.72(0.24)	3.01	0.002
							SS-LS	0.64(0.24)	3.21	0.007
			Max.rotation	–10.06(0.28)	35.35		SS-HS	–1.67(0.49)	–3.39	0.001
							SS-LS	–0.97(0.50)	2.83	0.049[$]
		Knee	Ave.rotation	8.96(0.27)	–32.70		SS-HS	1.07(0.45)	2.32	0.019[$]
							SS-LS	1.29(0.46)	3.00	0.005
		Ankle	Max.dorsiflexion/plantarflexion[#]	0.31(0.02)	–15.20		SS-HS	0.02(0.03)	0.91	0.361[$]
							SS-LS	0.07(0.03)	2.55	0.012
			Ave.dorsiflexion/plantarflexion[#]	0.17(0.01)	–32.79		SS-HS	0.02(0.10)	2.42	0.012
							SS-LS	0.02(0.10)	2.14	0.038[$]
	Left	Hip	Max.rotation	–20.03(0.23)	88.99		SS-HS	–1.92(0.74)	–2.52	0.010
							SS-LS	–1.82(0.76)	–2.60	0.016
			Ave.rotation	–5.87(0.06)	99.03		SS-HS	–0.58(0.22)	–2.65	0.007
							SS-LS	–0.54(0.22)	–2.66	0.013
CC	Right	Hip	Max.rotation	9.82(0.47)	–21.14	<0.05	SS-HS	1.72(0.66)	2.43	0.009
							SS-LS	0.70(0.67)	1.31	0.297[$]
		Knee	Max.extension/flexion	37.69(1.07)	–35.36		SS-HS	4.48(1.83)	2.35	0.015
							SS-LS	2.95(1.86)	0.64	0.114[$]
			Ave.extension/flexion	17.61(0.44)	–39.75		SS-HS	1.29(0.81)	1.56	0.112[$]
							SS-LS	2.03(0.82)	2.57	0.014
	Left	Hip	Max.adduction/abduction	–33.97(0.49)	69.57		SS-HS	–3.46(1.31)	–2.53	0.008
							SS-LS	–3.34(1.33)	–2.82	0.012
			Ave.adduction/abduction	–3.95(0.06)	59.89		SS-HS	–0.38(0.16)	–2.35	0.014
							SS-LS	–0.34(0.16)	–2.38	0.034[$]
		Knee	Ave.rotation	14.72(0.82)	–27.63		SS-HS	3.00(1.11)	2.16	0.007
							SS-LS	2.32(1.13)	2.49	0.040[$]

Note: EC: eccentric contraction; CC: concentric contraction; MD: mean difference; SE: standard error; Max: maximum; Min: minimum; Ave: average; [$]: without statistically significant difference ($p > 0.0167$); [#]: $\times 10^{-3}$.

biomechanics without increasing physiological cost. The adaptive LBS condition produced significantly higher shooting accuracy and a greater number of successful shots than the fixed-stiffness control conditions, while HR and SmO_2 remained comparable across conditions. Biomechanical analyses further indicated that athletes wearing adaptive footwear maintained advantageous lower-limb joint kinematics (ankle, knee, hip) under fatigue, suggesting that real-time stiffness regulation helped preserve more stable movement patterns.

These outcomes align with and extend existing literature on footwear stiffness and sports performance, which has largely examined fixed bending stiffness conditions. In basketball-specific tasks, carbon-plated or rigid midsole designs have not consistently improved jump height, yet they can meaningfully alter propulsion-related mechanics (e.g., increased ankle power/work, reduced ground contact time, increased take-off velocity) and foot–ankle kinematics/plantar loading patterns [24–26]. In running, systematic reviews generally report positive associations between higher LBS and improved economy (e.g., reduced oxygen cost) [27], and advanced carbon-plated footwear has produced modest but practically meaningful performance gains in elite competitions [28, 29]. Collectively, these findings suggest that stiffness can be beneficial, but its effects are task- and context-dependent; the present results extend this view by demonstrating that stiffness delivered adaptively during fatigue can enhance a complex, accuracy-sensitive basketball skill without additional physiological demand.

Notably, the present study differs from prior investigations by dynamically adjusting footwear stiffness in real time based on athlete biomechanics rather than maintaining static stiffness conditions. Previous studies by Healey and Hoogkamer [30] have typically used comparative static stiffness approaches or post-manufacture stiffness modifications. By contrast, the current system uses a lightweight, interpretable machine learning controller (logistic regression with SVM-RFE feature selection) to infer movement-state changes and adjust LBS online, enabling instantaneous feedback control. Comparable dynamic control concepts have been transformative in wearable technology applications such as smart exoskeletons and responsive insoles [31]. This dynamic adaptation may yield cumulative benefits across repeated actions, potentially explaining why we observed clearer performance enhancement than reports by Beltran et al. [32] showing limited effects with fixed carbon inserts in older runners or those by Healey and Hoogkamer [30] showing negligible changes in energy savings when carbon plates were removed from advanced running shoes. This alignment between pre-test discriminative biomechanics and post-test adaptive outcomes is consistent with model-guided intervention logic reported in predictive decision-support pipelines [20]. A leave-one-feature-out ablation further supported the selected feature set, as excluding LS_{EC} primarily reduced sensitivity while excluding t_{EC}/t_{CC} reduced specificity, indicating complementary roles in balancing classification performance.

Biomechanically, adaptive LBS likely supports task-specific elastic energy storage and return by modulating forefoot/MTP mechanics during propulsion. Willwacher et al. [33] demonstrated increased positive work and reduced negative work at the MTP joint in stiffer footwear, indicating recycling of stored elastic energy for propulsion. Riddick et al. [34] similarly reported reductions in plantar-flexor activation and ankle joint work using a foot-stiffening extending device during hopping, consistent with load redistribution from muscle to passive structures. In the present setting, increasing stiffness when fatigue-related biomechanical cues emerge may help maintain propulsive effectiveness and shooting execution without additional metabolic burden, consistent with the observed physiological neutrality.

Lower-limb kinematics further support the advantages of adaptive stiffness. Under fatigue, athletes often adopt compensatory and less optimal postures that can degrade accuracy. In this study, participants wearing adaptive shoes maintained more favorable joint kinematics throughout the fatiguing task, which likely stabilized their shooting mechanics. Prior work by Brini et al. [35] has linked consistency in key biomechanical patterns to shooting accuracy. Thus, adaptive stiffness may help sustain intended motor patterns by reducing fatigue-related variability.

Some discrepancies with previous findings warrant consideration. Evidence on fatigue and accuracy is mixed: earlier studies by Brini et al. [35] reported minimal post-fatigue accuracy decline, whereas more recent work by Daub et al. [36]—including the current research program—demonstrates accuracy reductions under physical and cognitive fatigue. Our results indicate that adaptive footwear may counteract such fatigue-related decrements. Likewise, running studies range from improved economy with stiff plates [37] to minimal or no improvements in some comparisons [30]. Differences in task specificity, participant demographics, and stiffness configurations likely explain these inconsistencies; for example, Beltran et al. [32] examined older runners with rear-foot striking patterns, which differ fundamentally from the current young athlete cohort performing basketball-specific movements.

Several limitations should be acknowledged. The modest sample size and specific athlete population may limit generalizability [38]. The controlled indoor environment and short protocol do not fully replicate competitive conditions involving prolonged exertion, multidirectional sequences, and psychological pressure [38, 39]. Moreover, the short-duration protocol does not capture potential user adaptation (habituation/learning) to stiffness modulation or cumulative fatigue effects that may emerge with prolonged use of the adaptive system [38, 40]. Longitudinal studies are therefore needed to examine whether performance benefits are sustained across repeated sessions and to evaluate long-term comfort, safety, and potential behavioral compensation [40]. The pretrained stiffness-adjustment algorithm may benefit from further subject-specific calibration [39]. In addition, electromyography (EMG) and detailed physiological fatigue markers were not collected, limiting mechanistic inference [40]. Finally, the scope focused on shooting performance, leaving other basketball skills unexamined [38].

Beyond basketball performance, the proposed biomechanical-signal-driven, AI-enabled adaptive control framework can be generalized to other human-centered domains that require real-time regulation of mechanical assistance [41]. Methodologically, this parallels interpretable AI decision-support systems in biomedical and risk-assessment contexts, where lightweight models and transparent feature attribution can facilitate trustworthy deployment in safety-relevant settings. In rehabilitation, the same sensing–inference–actuation paradigm could be used to tune orthotic stiffness or foot–ankle assistance profiles according to a patient's movement quality and fatigue state during gait retraining [41]. For assistive devices, lightweight and interpretable controllers similar to the present approach could support responsive exoskeleton or smart insole systems that modulate support levels across tasks while maintaining transparency and safety [41]. In occupational ergonomics, adaptive footwear or lower-limb support systems could dynamically adjust stiffness/support to mitigate cumulative fatigue, reduce overuse risk, and help sustain task performance during prolonged standing, walking, or manual handling [39]. These extensions

emphasize that the key contribution is a practical, interpretable closed-loop personalization architecture rather than a single sport-specific implementation.

Extending the proposed framework to other sports or movement tasks would follow a clear pathway: defining task-specific objectives (e.g., sprint acceleration, cutting efficiency, landing stability, or injury-risk proxies), selecting biomechanical signals that are most sensitive to fatigue-related performance degradation, and retraining the controller to map these signals to appropriate parameter updates (e.g., stiffness magnitude, timing, or support/damping profiles) [40]. For example, the same closed-loop paradigm could be adapted for repeated sprint–cut sequences in soccer, jump–landing tasks in volleyball, rapid stop-and-go movements in racket sports, or change-of-direction drills in court sports [40]. Such task-level extensions would help establish adaptive footwear and lower-limb systems as a general platform for human-in-the-loop performance support across diverse movement contexts.

Overall, this research supports the efficacy of dynamically adaptive LBS footwear driven by a biomechanical-signal-based machine learning controller for enhancing performance beyond static footwear designs without increasing physiological load. Future studies should evaluate the system in longer, game-like settings, incorporate richer biometric inputs like EMG or eye tracking, and test broader demographic groups and skill domains [38, 40]. These extensions could further establish responsive footwear as a practical platform for performance enhancement and injury-mitigation research in sports science and wearable technology.

4.9. Conclusion

Dynamically adjustable LBS footwear outperformed conventional high- and low-stiffness shoes in a 2-min basketball shooting–rebounding drill, delivering higher shot counts and accuracy while preserving lower-limb kinematics and incurring no additional cardiovascular or metabolic load. These findings confirm that real-time stiffness modulation can translate mechanical theory into practical performance gains and may mitigate fatigue-related injury risk. Although the sample was moderate and testing occurred in a controlled setting with a single adaptation algorithm, the results lay a foundation for wider trials in game environments, broader athlete populations, and more sophisticated control strategies. Adaptive LBS technology thus represents a promising direction for intelligent, task-responsive sports footwear.

Funding Support

This study was sponsored by the National Key R&D Program of China (2024YFC3607305), National Social Science Fund of China (25BTY103), Joint Fund of the Zhejiang Provincial Natural Science Foundation of China (LKLY26H170001), Zhejiang Provincial Key Project of Education Science Planning (2025SB084), Zhejiang Engineering Research Center for New Technologies and Applications of Helium-Free Magnetic Resonance Imaging Open Fund Project 2024 (2024GCPY02, 2024GCPY06), Scientific Research Fund of the Zhejiang Provincial Education Department (Y202559510), Ningbo Key Research and Development Program (2022Z196), Zhejiang Rehabilitation Medical Association Scientific Research Special Fund (ZKKY2023001), Research Academy of Medicine Combining Sports, Ningbo (No. 2023001), Ningbo Clinical Research Center for Orthopedics and Exercise Rehabilitation (No. 2024L004), and K. C. Wong Magna Fund in Ningbo University.

Conflicts of Interest

The authors declare that they have no conflicts of interest to this work.

Ethical Statement

The study was approved by the Ethics Committee of the Faculty of Sports Science, Ningbo University (Approval Number: TY202582). Written informed consent was obtained from all participants prior to participation.

Data Availability Statement

The data that support the findings of this study are openly available in the supplementary files of this article.

Author Contribution Statement

Yining Xu: Conceptualization, Methodology, Formal analysis, Investigation, Resources, Data curation, Writing – original draft, Visualization. **Yang Song:** Conceptualization, Methodology, Formal analysis, Investigation, Resources, Data curation, Writing – original draft, Visualization. **Dong Sun:** Conceptualization, Validation, Writing – review & editing, Supervision, Project administration, Funding acquisition. **Zhiyi Zheng:** Conceptualization, Methodology, Formal analysis, Investigation, Resources, Data curation, Writing – original draft, Visualization. **Mingwei Sun:** Conceptualization, Methodology, Formal analysis, Investigation, Resources, Data curation, Writing – original draft, Visualization. **Wenlong Li:** Methodology, Software, Writing – review & editing. **Jiachao Cai:** Methodology, Software, Writing – review & editing. **Xuanzhen Cen:** Methodology, Software, Writing – review & editing. **Zixiang Gao:** Methodology, Software, Writing – review & editing. **Liangliang Xiang:** Methodology, Software, Writing – review & editing. **Monèm Jemni:** Methodology, Software, Writing – review & editing. **Yaodong Gu:** Conceptualization, Validation, Writing – review & editing, Supervision, Project administration, Funding acquisition.

References

[1] Sayyadi, P., Minoonejad, H., Seidi, F., Shikhhoseini, R., & Arghadeh, R. (2024). The effectiveness of fatigue on repositioning sense of lower extremities: Systematic review and meta-analysis. *BMC Sports Science, Medicine and Rehabilitation*, *16*(1), 35. https://doi.org/10.1186/s13102-024-00820-w

[2] Taylor, J. L. I., & Burkhart, T. A. (2025). Tired of ACL injuries: A review of methods and outcomes of neuromuscular fatigue as a risk factor for ACL injuries. *Biomechanics*, *5*(1), 11. https://doi.org/10.3390/biomechanics5010011

[3] Rodrigo-Carranza, V., González-Mohíno, F., Santos-Concejero, J., & González-Ravé, J. M. (2022). The effects of footwear midsole longitudinal bending stiffness on running economy and ground contact biomechanics: A systematic review and meta-analysis. *European Journal of Sport Science*, *22*(10), 1508–1521. https://doi.org/10.1080/17461391.2021.1955014

[4] Worobets, J., & Wannop, J. W. (2015). Influence of basketball shoe mass, outsole traction, and forefoot bending stiffness on

three athletic movements. *Sports Biomechanics*, *14*(3), 351–360. https://doi.org/10.1080/14763141.2015.1084031

[5] Reis, F. J. J., Alaiti, R. K., Vallio, C. S., & Hespanhol, L. (2024). Artificial intelligence and machine learning approaches in sports: Concepts, applications, challenges, and future perspectives. *Brazilian Journal of Physical Therapy*, *28*(3), 101083. https://doi.org/10.1016/j.bjpt.2024.101083

[6] Gandhi, V., Chaudhari, Y., Kumar, A., Revakar, H., Oza, A. D., & Yadav, S. L. (2026). Benchmarking machine learning models for obesity classification with SHAP-based interpretability. *International Journal of Computational Intelligence Systems*, *19*(1), 8. https://doi.org/10.1007/s44196-025-01078-x

[7] Gandhi, V. C., Gandhi, P., Ogundiran, J. O., Tshibola, M. S. S., & Kapuya Bulaba Nyembwe, J.-P. (2025). Computational modeling and optimization of deep learning for multi-modal glaucoma diagnosis. *AppliedMath*, *5*(3), 82. https://doi.org/10.3390/appliedmath5030082

[8] Hoogkamer, W., Kipp, S., Frank, J. H., Farina, E. M., Luo, G., & Kram, R. (2018). A comparison of the energetic cost of running in marathon racing shoes. *Sports Medicine*, *48*(4), 1009–1019. https://doi.org/10.1007/s40279-017-0811-2

[9] Joseph, A. M., Kian, A., & Begg, R. (2024). Enhancing intelligent shoes with gait analysis: A review on the spatiotemporal estimation techniques. *Sensors*, *24*(24), 7880. https://doi.org/10.3390/s24247880

[10] Tunca, C., Pehlivan, N., Ak, N., Arnrich, B., Salur, G., & Ersoy, C. (2017). Inertial sensor-based robust gait analysis in non-hospital settings for neurological disorders. *Sensors*, *17*(4), 825. https://doi.org/10.3390/s17040825

[11] D'Alcala, E. R., Voerman, J. A., Konrath, J. M., & Vydhyanathan, A. (2021). *Xsens DOT wearable sensor platform white paper. [White paper]. Movella*. https://www.movella.com/hubfs/Downloads/Whitepapers/Xsens%20DOT%20WhitePaper.pdf

[12] Erer, K. S. (2007). Adaptive usage of the Butterworth digital filter. *Journal of Biomechanics*, *40*(13), 2934–2943. https://doi.org/10.1016/j.jbiomech.2007.02.019

[13] Chaaban, C. R., Berry, N. T., Armitano-Lago, C., Kiefer, A. W., Mazzoleni, M. J., & Padua, D. A. (2021). Combining inertial sensors and machine learning to predict vGRF and knee biomechanics during a double limb jump landing task. *Sensors*, *21*(13), 4383. https://doi.org/10.3390/s21134383

[14] Guyon, I., Weston, J., Barnhill, S., & Vapnik, V. (2002). Gene selection for cancer classification using support vector machines. *Machine Learning*, *46*(1), 389–422. https://doi.org/10.1023/A:1012487302797

[15] Lundberg, S. M., & Lee, S.-I. (2017). A unified approach to interpreting model predictions. In *Proceedings of the 31st International Conference on Neural Information Processing Systems*, 4768–4777.

[16] Kang, H. (2021). Sample size determination and power analysis using the G*Power software. *Journal of Educational Evaluation for Health Professions*, *18*, 17. https://doi.org/10.3352/jeehp.2021.18.17

[17] Yanhao, S., Hengsuko, E., & Promthep, K. (2024). The construction of evaluation model for analyzing basketball player performance based on fuzzy comprehensive evaluation method. *Journal of Roi Kaensarn Academi*, *9*(10), 593–603.

[18] Schaffarczyk, M., Rogers, B., Reer, R., & Gronwald, T. (2022). Validity of the Polar H10 sensor for heart rate variability analysis during resting state and incremental exercise in recreational men and women. *Sensors*, *22*(17), 6536. https://doi.org/10.3390/s22176536

[19] Jaén-Carrillo, D., Roche-Seruendo, L. E., Cartón-Llorente, A., & García-Pinillos, F. (2021). Agreement between muscle oxygen saturation from two commercially available systems in endurance running: Moxy Monitor versus Humon Hex. *Proceedings of the Institution of Mechanical Engineers, Part P: Journal of Sports Engineering and Technology*, *236*(3), 231–237. https://doi.org/10.1177/17543371211015764

[20] Gandhi, V. C., Thakkar, D., & Milanova, M. (2025). Unveiling Alzheimer's progression: AI-driven models for classifying stages of cognitive impairment through medical imaging. In *Pattern Recognition. ICPR 2024 International Workshops and Challenges: International Conference on Pattern Recognition 2024*, 55–87. https://doi.org/10.1007/978-3-031-88220-3_4

[21] Thakar, S., Patel, D., Gandhi, V. C., & Trivedi, D. (2024). Financial analytics with artificial neural networks: Predicting loan repayment. In *International Conference on I-SMAC (IoT in Social, Mobile, Analytics and Cloud)*, 1667–1673. https://doi.org/10.1109/I-SMAC61858.2024.10714849

[22] Katlariwala, S. B., Gandhi, V. C., Patel, N., Parmar, D., & Desai, A. (2025). TriBoost and beyond: Advanced machine learning approaches for diabetes risk prediction. In *International Conference on Electronics and Renewable Systems*, 1780–1785. https://doi.org/10.1109/ICEARS64219.2025.10941310

[23] Küderle, A., Ullrich, M., Roth, N., Ollenschläger, M., Ibrahim, A. A., Moradi, H., . . . , & Eskofier, B. M. (2024). Gaitmap—An open ecosystem for IMU-based human gait analysis and algorithm benchmarking. *IEEE Open Journal of Engineering in Medicine and Biology*, *5*, 163–172. https://doi.org/10.1109/OJEMB.2024.3356791

[24] Jia, S.-W., Yang, F., Wang, Y., Guo, T., & Lam, W.-K. (2022). Shoe bending stiffness influence on lower extremity energetics in consecutive jump take-off. *Applied Bionics and Biomechanics*, *2022*(1), 5165781. https://doi.org/10.1155/2022/5165781

[25] Bourdas, D. I., Travlos, A. K., Souglis, A., Gofas, D. C., Stavropoulos, D., & Bakirtzoglou, P. (2024). Basketball fatigue impact on kinematic parameters and 3-point shooting accuracy: Insights across players' positions and cardiorespiratory fitness associations of high-level players. *Sports*, *12*(3), 63. https://doi.org/10.3390/sports12030063

[26] Cao, S., Geok, S. K., Roslan, S., Sun, H., Lam, S. K., & Qian, S. (2022). Mental fatigue and basketball performance: A systematic review. *Frontiers in Psychology*, *12*, 819081. https://doi.org/10.3389/fpsyg.2021.819081

[27] Pernigoni, M., Ferioli, D., Calleja-González, J., Sansone, P., Tessitore, A., Scanlan, A. T., & Conte, D. (2024). Match-related fatigue in basketball: A systematic review. *Journal of Sports Sciences*, *42*(18), 1727–1758. https://doi.org/10.1080/02640414.2024.2409555

[28] Bernuz, B., Laujac, S., Sirial, C., Auffret, S., Preda, C., Slawinski, J., . . . , & Gavarry, O. (2024). Effect of advanced footwear technology spikes on sprint acceleration: A multiple N-of-1 trial. *Sports Medicine—Open*, *10*(1), 92. https://doi.org/10.1186/s40798-024-00758-w

[29] Rodrigo-Carranza, V., Gonzalez-Mohino, F., Santos Del Cerro, J., Santos-Concejero, J., & Gonzalez-Rave, J. M. (2021). Influence of advanced shoe technology on the top 100 annual performances in men's marathon from 2015 to

2019. *Scientific Reports*, *11*(1), 22458. https://doi.org/10.1038/s41598-021-01807-0

[30] Healey, L. A., & Hoogkamer, W. (2022). Longitudinal bending stiffness does not affect running economy in Nike Vaporfly shoes. *Journal of Sport and Health Science*, *11*(3), 285–292. https://doi.org/10.1016/j.jshs.2021.07.002

[31] Espinosa, H., Mears, A., Stamm, A., Ohgi, Y., & Coniglio, C. (2025). Wearable sensor technology in sports monitoring. *Sports Engineering*, *28*(1), 4. https://doi.org/10.1007/s12283-025-00485-9

[32] Beltran, R. T., Powell, D. W., Greenwood, D., & Paquette, M. R. (2023). The influence of footwear longitudinal bending stiffness on running economy and biomechanics in older runners. *Research Quarterly for Exercise and Sport*, *94*(4), 1062–1072. https://doi.org/10.1080/02701367.2022.2114589

[33] Willwacher, S., Konig, M., Potthast, W., & Bruggemann, G.-P. (2013). Does specific footwear facilitate energy storage and return at the metatarsophalangeal joint in running? *Journal of Applied Biomechanics*, *29*(5), 583–592. https://doi.org/10.1123/jab.29.5.583

[34] Riddick, R. C., Farris, D. J., Brown, N. A. T., & Kelly, L. A. (2021). Stiffening the human foot with a biomimetic exotendon. *Scientific Reports*, *11*(1), 22778. https://doi.org/10.1038/s41598-021-02059-8

[35] Brini, S., Delextrat, A., & Bouassida, A. (2021). Variation in lower limb power and three-point shot performance following repeated sprints: One vs five changes of direction in male basketball players. *Journal of Human Kinetics*, *77*, 169–179. https://doi.org/10.2478/hukin-2021-0019

[36] Daub, B. D., McLean, B. D., Heishman, A. D., Peak, K. M., & Coutts, A. J. (2024). The relationship between mental fatigue and shooting performance over the course of a National Collegiate Athletic Association Division I basketball season. *The Journal of Strength & Conditioning Research*, *38*(2), 334–341. https://doi.org/10.1519/JSC.0000000000004624

[37] Xu, L., Wang, Y., & Wen, X. (2025). The role of footwear in improving running economy: A systematic review with meta-analysis of controlled trials. *Scientific Reports*, *15*(1), 3963. https://doi.org/10.1038/s41598-025-88271-2

[38] Lin, H.-T., Kuo, W.-C., Chen, Y., Lo, T.-Y., Li, Y.-I., & Chang, J.-H. (2022). Effects of fatigue in lower back muscles on basketball jump shots and landings. *Physical Activity and Health*, *6*(1), 273–286. https://doi.org/10.5334/paah.199

[39] Song, Y., Cen, X., Wang, M., Gao, Z., Tan, Q., Sun, D., …, & Zhang, M. (2025). A systematic review of finite element analysis in running footwear biomechanics: Insights for running-related musculoskeletal injuries. *Journal of Sports Science & Medicine*, *24*, 370–38. https://doi.org/10.52082/jssm.2025.370

[40] Yu, P., & Fernandez, J. (2024). Alterations in lower limb biomechanical characteristics during the cutting manoeuvre in chronic ankle instability population and copers. *Physical Activity and Health*, *8*(1), 148–156. https://doi.org/10.5334/paah.380

[41] Sarma, J., Sahai, N., & Bhatia, D. (2020). Recent advances on ankle foot orthosis for gait rehabilitation: A review. *International Journal of Biomedical Engineering and Technology*, *33*(2), 159–173. https://doi.org/10.1504/IJBET.2020.107711

How to Cite: Xu, Y., Song, Y., Sun, D., Zheng, Z., Sun, M., Li, W., …, & Gu, Y. (2026). Adaptive Footwear Stiffness Driven by Biomechanical Signals for Improving High-Intensity Metabolic-Neuromuscular Performance: A Randomized Controlled Trial. *Artificial Intelligence and Applications*. https://doi.org/10.47852/bonviewAIA62028408